

# LINAC EXPERIENCE IN THE FIRST TWO YEARS OF OPERATION @ CNAO (CENTRO NAZIONALE ADROTERAPIA ONCOLOGICA)

S. Vitulli, E. Vacchieri, CNAO Foundation, Pavia, Italy  
 A. Reiter, B. Schlitt, GSI, Darmstadt, Germany

## Abstract

CNAO is the first medical accelerator facility for deep hadrontherapy with protons and carbon ions in Italy. The LINAC injector at CNAO, entirely built by the GSI and Frankfurt University collaboration, is equal to the HIT LINAC working in the hadrontherapy centre of Heidelberg, Germany [3]. It includes a four-rod type RFQ structure accelerating up to 400 keV/u and an IH structure to increase the energy up to 7 MeV/u. Such LINAC works as injector in a 78 m circumference synchrotron where the protons and carbon beams reach respectively 250 MeV/u and 400 MeV/u. The LINAC commissioning was performed during 2009 and from beginning of 2011 it entered into routine and continuous operation (24hrs, 7days). First patient was treated in September 2011. Maintenance periods are foreseen three times per year. Different diagnostic elements are installed along the injection line, like profile grids, faraday cups, current transformers, capacitive pick-ups. The principal parameters are daily monitored, like output energy by means of online not destructive ToF measurements, cavities voltage, cavities RF forward power and beam current transmission. No major faults were observed in the first two years of operation. LINAC beam energy is stable within 0.02 MeV/u on a typical value of 7.17 MeV/u. The relation between LINAC extraction and synchrotron injection is under investigation. This paper summarizes the monitoring issues (i.e. reproducibility of settings and beam parameters as well as long term stability measures) on the CNAO LINAC during daily patient treatments and outlines the measurements performed in the initial commissioning compared within actual status.

CNAO machine is depicted in Fig.1.

Particles originate from one of the two Electron Cyclotron Resonance (ECR) sources, producing either  $C^{4+}$  or  $H^{3+}$  ions, at 8keV/u; they travel along the LEBT line and the LINAC reaching 7MeV/u energy and pass through the Medium Energy Beam Transfer (MEBT) line where a debuncher cavity is placed in order to reduce the beam energy dispersion. Then particles are accelerated in a 25m diameter synchrotron and, finally, are extracted into one of the four extraction lines, delivering either  $C^{6+}$  or proton beam to one of the three treatment rooms.

Extraction energy depends on treatment requirements: the deeper is the tumour to be irradiated, the higher is the required energy. Extraction energy can vary from 120 to 400MeV/u for Carbon ions and from 60 to 250MeV/u for protons. Extraction process is of the order of one second.

Actually beam maximum intensity at patient is  $5 \cdot 10^9$  and  $1 \cdot 10^8$  particles/s per spill, for protons and Carbon ions respectively. It can be reduced up to a factor 10, by inserting pepper-pot filters in the MEBT line and extracting the beam with spills over a longer extraction time.

## THE CNAO MEDICAL EXPERIENCE

From September 2011, 21 patients were treated with protons with an average of 6 patient/day and 35 treatment sessions/patient [1]. Each session is done by two different fields with different irradiation angles for a total of about 10-15 minutes of beam irradiation. The selected cases are principally chordoma (16 patients) and chondrosarcoma (5 patients) tumours in the head-neck (13 patients) or pelvis (8 patients) districts.

For head and neck tumors, solid mask, bite block, infrared-reflecting markers are used for patients fixing into couch. For pelvis tumors, the patient is fixed by means thermoplastic body mask. The dose uniformity is within the requested limit of  $\pm 2.5\%$ .

Today all the 148 foreseen energies are applied for treatments, one room is used with proton beams and with a fixed spot size of 1 cm using a couch for patient positioning.

During next year it will be possible to work all the three rooms, including the vertical line, with variable spot size of proton and carbon ions; in the treatment room both chair and couch for patient positioning will be available.

## THE LINAC INJECTOR

The layout of the CNAO injector includes two ECR ion sources and the LEBT [5]. A particularity of the CNAO

## THE CNAO MACHINE

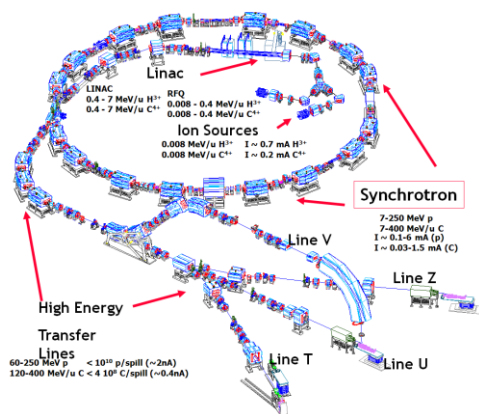


Figure 1: Sketch of the CNAO machine complex.

injection line is to be placed inside the synchrotron resulting a more compact accelerator machine.



Figure 2: RFQ and IH structure in synchrotron room.

A switching dipole magnet merges the two source lines into one. After being bent by a 75°-dipole, the beam enters the RFQ and the IH structure (Fig.2), after the so called intermatching section containing two quadrupoles for focusing and two steerers (horizontal and vertical) for moving the beam (Fig.3).

Also inside the IH-DTL tank there are three magnetic quadrupole triplet lenses for transverse focusing and another triplet behind the tank [4].

Upstream the RFQ, an electrostatic deflector (*Chopper*) is installed. The beam is continuous from the sources to the chopper, while it is pulsed downstream (i.e., 50-100us pulse).

Along the LEBT, three solenoids, four dipoles, eleven quadrupoles and correctors are used to focus, bend and steer the beam.

As concerns beam diagnostics, an AC transformer for non destructive current measurement is placed before the stripper foil chamber [2].

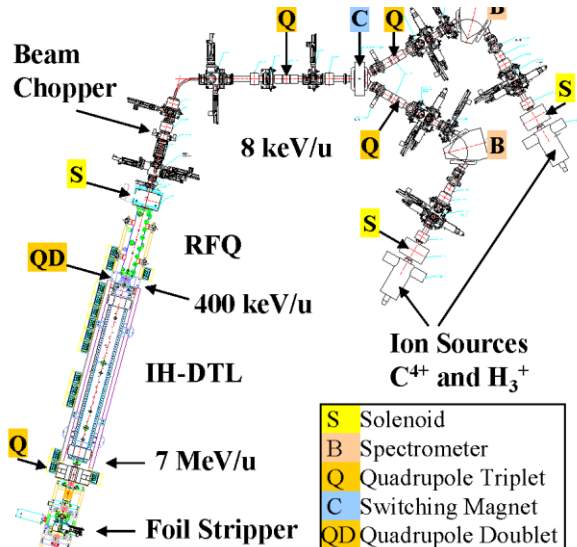


Figure 3: LINAC injector layout. Sketch of magnets and beam diagnostics tanks, from the sources to the stripper tank.

Inside the RFQ and IH structures two tank probes are placed in order to check the RF signal in any time (Fig. 4b).

After the IH structure, along the MEBT line, there are two phase probes @ 3478 mm distance for Time-Of-Light measurements (Fig. 4a), six profile grids for position monitoring and three faraday cups. All the diagnostic devices were delivered by GSI [3,4,9].

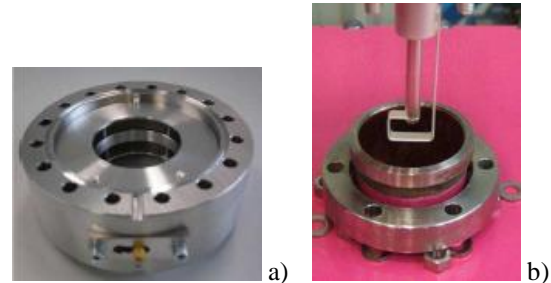


Figure 4: a) Phase probe for beam measurements (installed on the beam line) b) Tank probe for RF measurements (on the top of the corresponding flange in the IH tank).

At the end of the LINAC line, the stripping foil allows scratching the remaining electrons producing a defined charge state (from  $H^{3+}$  to 3 protons; from  $C^{4+}$  to  $C^{6+}$ ). In Table1 the main LINAC Design Parameters are reported.

Table 1: Main LINAC Parameters

Physical Parameters	Values
Beam particle species	$H^{3+}$ , $C^{4+}$
Operation frequency	216.816 MHz
RFQ injection beam energy	8 keV/u
Final LINAC beam energy	7 MeV/u
Beam pulse length	$\leq 300 \mu s$
Beam repetition rate	$\leq 5$ Hz
Stability pulse repetition rate	10 Hz
Exit beam energy spread <sup>1</sup>	$\leq \pm 0.4 \%$
Total LINAC length <sup>2</sup>	6.95 m

<sup>1</sup> straggling effect in the stripper foil not included

<sup>2</sup> including RFQ, IH and Stripper section

## LINAC COMMISSIONING

CNAO LINAC commissioning took place during 2009 as listed in Table 2.  $H_{3+}$  and  $C_{4+}$  ion beams have been used for all beam commissioning phases [6, 7]. The first turn in the synchrotron was achieved in December 2009.

Table 2: Main CNAO LINAC commissioning steps

Date	Activity
Jan 09	RFQ installation
Feb-Mar 09	RFQ RF conditioning
Mar 12 <sup>th</sup> – Apr 3 <sup>rd</sup>	Beams @ 400 keV/u
Apr 09	IH installation
May-Jun 09	IH RF conditioning
Jun 22 <sup>th</sup> – Jul 15 <sup>th</sup>	Beams 7 MeV/u
Jul-Nov 09	Completion of the line
Nov-Dic 09	$H^{3+}$ beam @ MEBT end
Dic 09	$H^{3+}$ first turn in synchrotron

Three different beam diagnostics test benches were used behind LEBT, behind RFQ, and behind the stripper section, respectively, and allowed for beam current, profile, and emittance measurements. Final LINAC test bench contained three phase probes at known distance for accurate Time-of-Flight measurements; a profile grid; two faraday cups and one AC transformer in addition to a mobile emittance device, that is a slit-grid measurement system.

More than 140 measurement series including numerous amplitude, phase, and emittance scans were performed with the IH-DTL. Different LEBT beam energies, RFQ settings, and IH tank RF plunger configurations were investigated.

The LINAC was optimized with respect to high beam transmission, minimum beam emittances and optimized bunch signal amplitudes from the phase probes.

Phase and voltage of RFQ and IH scans were done monitoring the variation of the above mentioned parameters. The RFQ phase is kept fix as reference point.

The current transmission reaches a maximum for determined values of IH phase and voltage as is shown in Fig. 5 and Fig. 6.

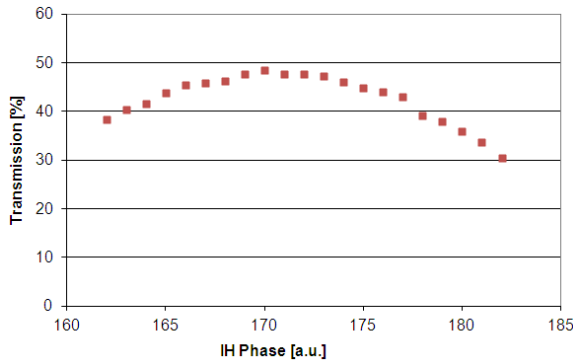


Figure 5:  $C^{4+}$ : IH phase scan as a function of the total LINAC transmission. Settings:  $V_{RFQ} = 5.1V$ ;  $V_{IH} = 5.7V$ .

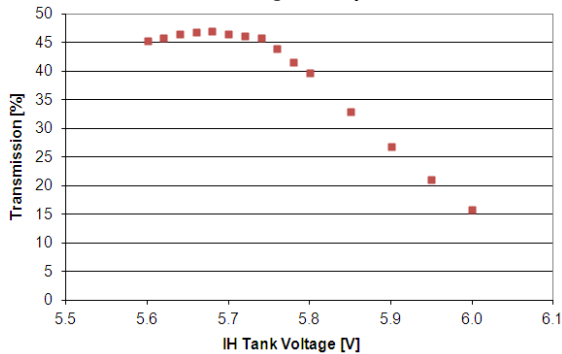


Figure 6:  $C^{4+}$ : IH Voltage scan as a function of the total LINAC transmission. Settings:  $V_{RFQ} = 5.1V$ ;  $\Phi_{IH} = 170$  a.u.

The beam energy can vary within 0.5% by changing RFQ and IH tank voltages or phases (Fig.7 and Fig.8). It means that little adjustments are possible for the future matching within the synchrotron injection. Fig. 7 and Fig. 8 shown the measurements taken by the Time-of-Light

method with the three phase probes installed along the test bench for IH commissioning. They are considered in pairs comparing the calculated energy to improve the measurement accuracy.

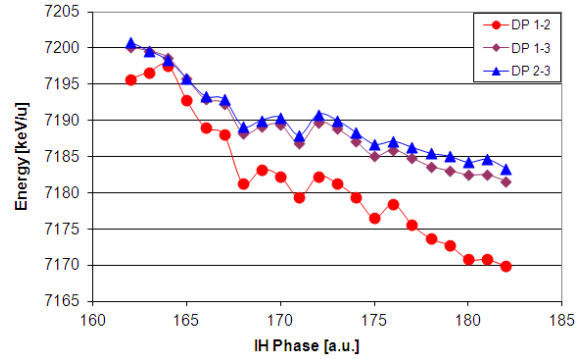


Figure 7:  $C^{4+}$ : IH phase scan as a function of the energy. Settings:  $V_{RFQ} = 5.1V$ ;  $V_{IH} = 5.7V$ . Legend: DP 1-2 = ToF between 1<sup>st</sup> end 2<sup>nd</sup> phps; DP 1-3 = ToF between 1<sup>st</sup> and 3<sup>rd</sup> phps; DP 2-3 = ToF between 2<sup>nd</sup> and 3<sup>rd</sup> phps.

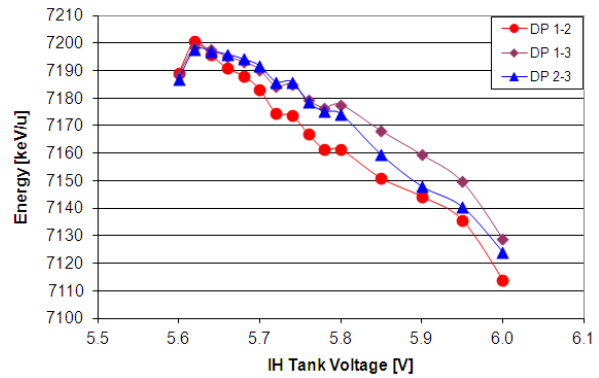


Figure 8:  $C^{4+}$ : RFQ and IH Voltage scan as a function of the energy. Settings:  $V_{RFQ} = 5.1V$ ;  $\Phi_{IH} = 170$  a.u. Legend like Fig. 7.

The experience shows that if the IH voltage increases, the beam energy increases too. On the opposite, if the IH phase increases, the energy decreases.

The final chosen working point corresponds to about 7.2 MeV/u at a RF pulse power of ~910 kW. Table 3 summarizes maximum beam currents achieved behind the stripping foil. Design beam currents were reached and even exceeded.

Table 3: Nominal and measured beam current @ LINAC exit

Request @ LINAC exit	Measured	Nominal
current for $C^{6+}$ (7 MeV/u)	135 $\mu$ A	120 $\mu$ A
current for p (7MeV/u)	1.2 mA	0.75 mA

The measured emittances after RFQ and IH are within the project values (for  $C^{6+}$ : 5.4  $\pi$ -mm-mrad horizontal and 4.2  $\pi$ -mm-mrad vertical plane; for  $H^{3+}$ : 6.8  $\pi$ -mm-mrad horizontal and 6.5  $\pi$ -mm-mrad vertical).

RFQ transmission around 60% has been measured for both  $H^{3+}$  and  $C^{4+}$  beams. The IH transmission, in

transport mode, which is without use IH structure as accelerator, is 100%; in acceleration mode is 80%. Finally the total maximum LINAC transmission is around 50% for  $C^{6+}$  and 45% for  $H^{3+}$ .

Beam profiles are taken along the MEBT by means of six profile grids. Typical beam shapes before and after the stripping foil are shown in Fig. 9. For optimization purposes the beam should be as centred as possible.

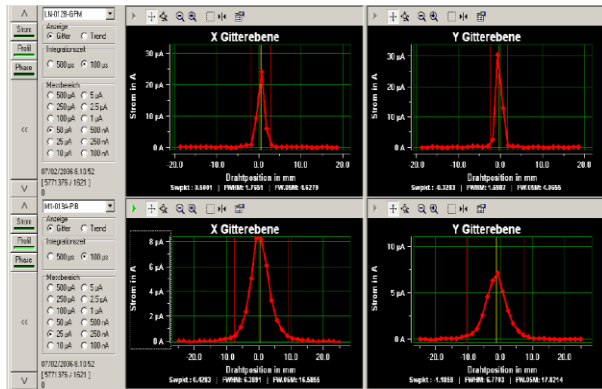


Figure 9: Beam Profiles before the stripping foil (LN-012B-GPM) and 1.3 m after the stripper (M1-019A-PIB) for carbon beam. Legend: GPM = GSI Profile Monitor, PIB = profile intensity in the MEBT line.

### DAILY LINAC MEASUREMENTS

In order to describe the behaviour of the CNAO LINAC machine a daily non invasive monitoring is done during the treatment sessions with proton beam.

RFQ, IH and debuncher voltages and phases are set by the control system, but the effective values can be checked continuously on the LINAC control system. Voltages are measured by the tank probe signals. RFQ and IH waveform are shown in Fig. 10. Peak-to-peak values are taken as indicative daily data, due to the limited accuracy of the digitizer, rather than more precise values can be measured directly from one of the RF amplifier outputs.

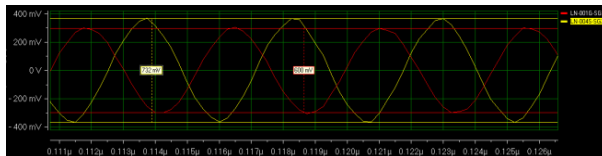


Figure 10:  $H^{3+}$ : RFQ and IH Voltage as measured from the tank probes. Settings: RFQ voltage = 5.29V; IH voltage = 5.72V.

The beam intensity is observed by the voltage of the phase probe along the MEBT line (M3-029A-PHP) rebuilt in Fig. 11 together with the debuncher tank probe signal.

The debuncher in fact is useful for optimizing the beam injection in the synchrotron. It is kept under control by the tank probe M3-012J-SG4 and its effect on the beam

bunches is evident on the phase probe mentioned above (Fig. 11). A confirm of the debuncher optimization is done changing its phase or voltage and observing a constant phase difference between M3-012J-SG4 and M3-029A-PHP. The effect of the debuncher is checked observing the bunch shapes with debuncher @ different set voltages (see Fig. 11).

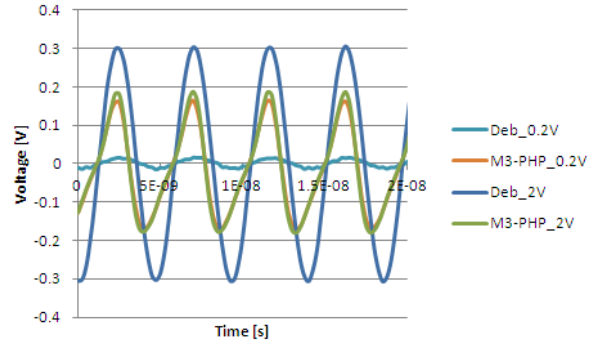


Figure 11: Debuncher tank signal and beam signal from the MEBT phase probe @ different debuncher set voltage @  $358^\circ$  difference phase respect to the IH phase.

The phase difference between the three RF structures is evaluated from a time calculation between the tank probes signals. It is important to monitor these phase differences in order to maintain a good match between them. The CNAO LINAC is well set in term of phase difference stability (see Fig. 12).

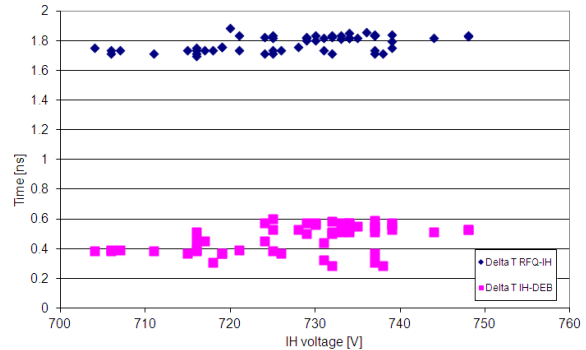


Figure 12:  $H^{3+}$ : Phase difference between the RF structures from January to June 2012.

The final beam energy is done by a ToF measurement between the two phase probes placed after the LINAC tank (Fig. 13).

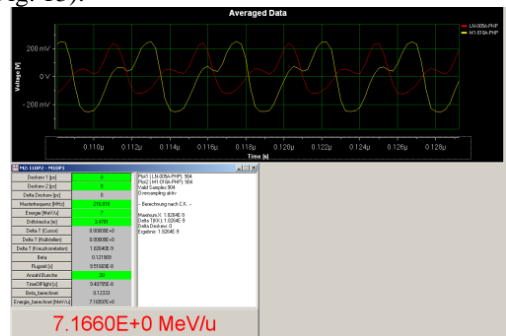


Figure 13:  $H^{3+}$ : phase probes signals after the LINAC to calculate the ToF (IH voltage = 5.72V).

The energy outside then LINAC is strongly dependent on different parameters, not only on the IH voltage and phase, but even on the cooling water temperature that must be stable within 0.2°C.

The RF power is not adjusting, but it is a consequence of the set voltage. It can be read on the amplifier cabinet PLC.

### STABILITY LINAC MEASUREMENTS

Periodically energy, current and profile stability measurements for tens hours are foreseen in order to check beam parameters at the LINAC exit.

In terms of energy, a variability of 0.4% is normally acceptable.

In term of current, a variability of 2% does not normally causing troubles for a good injection (Fig. 14).

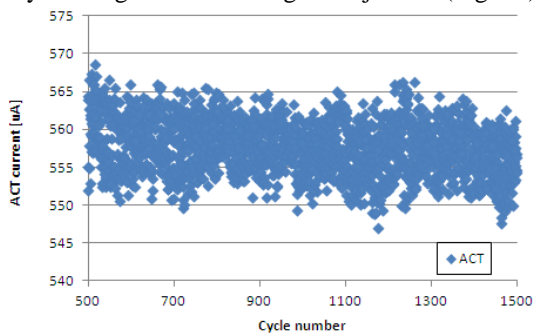


Figure 14: Beam current stability measurements from 00h39 to 10h01 of April 28, 2012.

The beam position along the MEBT line, after the LINAC tank, can be monitored by means of six profile grids (Fig. 15). Such interceptive measurements are done during the night shifts in order to assure the correct beam trajectory.

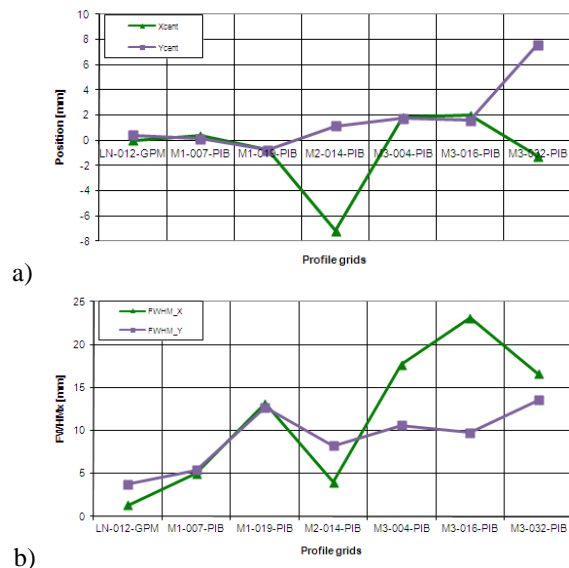


Figure 15: Beam position (a) and width (b) along the MEBT line measured by means of profile grids.

Position stability measurements are planned monthly in order to check the natural beam displacement along the MEBT that normally can reach 0.2mm for the position and 0.4mm for the FWHM.

### BEAM STUDIES IN SYNCHROTRON

Different measurements and trends were studied for understanding a possible involvement of the LINAC behaviour in the occasional instability of the intensity of the accelerated beam after the synchrotron RF cavity trapping [8]. Fig. 16 shows a typical beam spill in the synchrotron DCCT (DC-Current Transformer) that is analysed in order to optimize the injection and acceleration [10].

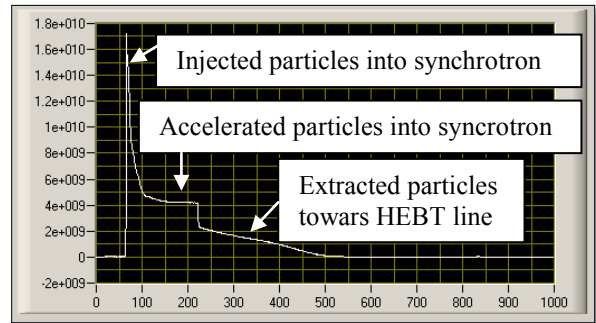


Figure 16: One synchrotron cycle (4.8s duration) as measured by the DC current transformer (acquisition rate: ~5ms/sample). The first peak corresponds to the particles injected in the synchrotron, the next plateau represents the particle accelerated from the RF cavity and the following drop is related to the beam extraction towards the HEBT line (1.3s duration).

The most related element is the debuncher cavity that is placed in the MEBT line as shown in Fig. 17.

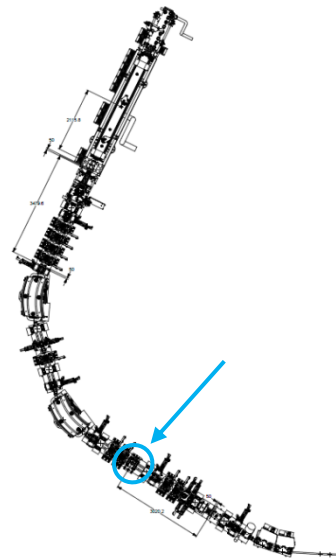


Figure 17: LINAC and MEBT layout showing the debuncher position and the distances between phase and tank probes.

Changing the debuncher phase influences beam energy distribution thus causing different synchrotron injections.

On the other hand, the debuncher voltage variation has not great influence on the energy distributions, as one can deduce from Fig. 18.

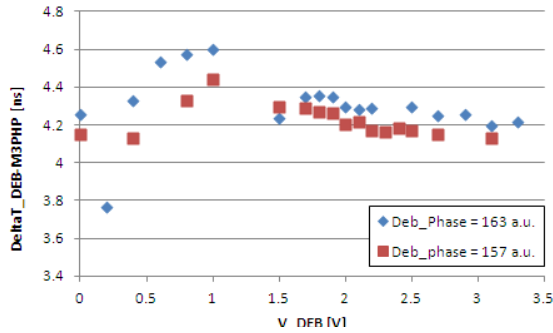


Figure 18: Phase difference between debuncher and MEBT phase probe as a function of the debuncher voltage.

Different scans in phase and voltage were done as a function of the DCCT signal. Fig. 19 shows a study around the typical values of the debuncher phase.

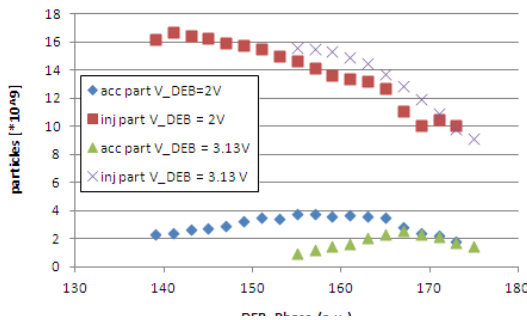


Figure 19: Particles injected and accelerated in the synchrotron as a function of the debuncher phase @ different typical values for the debuncher voltage.

Figure 20 shows the debuncher voltage study: one can deduce that it has not a great influence on the injected and accelerated particle number.

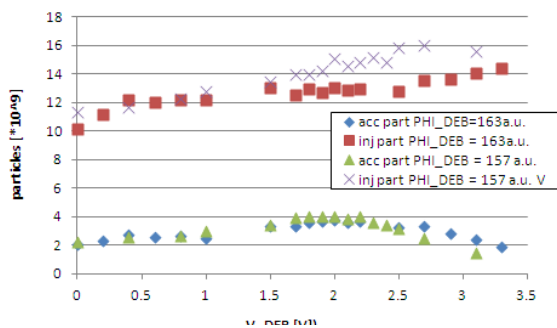


Figure 20: Particles injected and accelerated in the synchrotron as a function of the debuncher voltage @ different typical values for the debuncher phase.

## CARBON MEASUREMENTS

During the afternoon commissioning sessions the carbon beam is in preparation for obtaining the authorization to treat patients before the end of this year.

In term of LINAC injection, carbon beam has similar energy dispersion and even better transmission then proton beam.

## LINAC MAINTENANCE AND UPGRADE

During the last three years, the LINAC and its supply were running in a very reliable way. Only few breakdowns were caused by some hardware faults easily solved by upgrades or using the available spare parts.

For example a Variac transformer of the tetrode tube filament burned twice, much before the waiting usury time; the RFQ anode filter had a short circuit; the capacitor foils broke two time in two week (in both cases an electric discharge made a hole in the foils); some Low Level RF amplifier modules were sent to the producer for repair; some control board cards needed to be replaced in some parts.

In terms of upgrade, all the air filter system inside the RF cabinet was improved to preserve the cabinets from dust diseases; some flow meters were add in synchrotron room, one for each different element to be cooled; all the IGBT transistor cards in the LINAC magnets power supplies were modified mounting more reliable diodes.

The RF tetrode tubes never stop working. Only one was changed in order to verify the spare. IH tubes are around 13400 h working; RFQ tetrode is around 15700h.

Maintenance work is divided into six-monthly and annual activities and includes checks on the ventilation fans, on the flow meters, on the variac transformers, dust cleanness inside the cabinets, check of the electrical wiring, RF reference measurements. Most of these activities reclaim to switch off the machine and can be done only during the maintenance periods that are planned three times in a year.

During patient treatments very rarely breakdowns occur caused by LINAC faults. When it happens, the problem was mainly related to the control system and timing, so that a solution was possible in remote way without loss treatment but only interrupting it for some minutes.

## CONCLUSIONS

LINAC commissioning was done during 2009 finding the working point that corresponds to about 7.2 MeV/u energy at a RF pulse power of ~910 kW.

In the first two years of operation it was stable and reliable. Daily a complete summary of the measured parameters is done to check the correct beam position, energy, current and bunch shape. Same values, like IH e Debuncher voltage and phase, should be adjusted via control system to assure a good matching within the synchrotron that need the LINAC exit energy as initial parameter for an efficient RF cavity trapping and

acceleration. Stability measurements during the night shift have been done to guarantee the oscillation around the set values doesn't exceed the foreseen one. Some studies on the possible involvement of the LINAC parameters in occasional instabilities of the accelerated beam in the synchrotron have been done and shown that, in those cases, a more stable configuration can be reached varying the debuncher phase.

### REFERENCES

- [1] E.Bressi et al, Proc. IPAC2012, THXA02.
- [2] A.Parravicini et al., Proc. HIAT2009, p. 247.
- [3] B. Schlitt, Proc. LINAC2008, p. 720.
- [4] H. Vormann et al., Proc. EPAC2008, p. 1833.
- [5] E. Bressi et al., TU6PFP005.
- [6] P.A. Posocco et al., Proc. HIAT2009, p. 188.
- [7] B. Schlitt et al., Proc. IPAC2010, p. 67.
- [8] L. Falbo et al., Proc. IPAC2011, WEPS006.
- [9] A. Reiter, Proc. EPAC2006, p. 1028.
- [10] C. Priano et al., IPAC2011, WEPS007.